

Characterization and Peroxidase Activity of a Myoglobin Mutant Containing a Distal Arginine

Cristina Redaelli,^[a] Enrico Monzani,^[a] Laura Santagostini,^[a] Luigi Casella,^{*[a]}
Anna Maria Sanangelantoni,^[b] Roberta Pierattelli,^[c] and Lucia Banci^[c]

The spectroscopic, conformational, and reactivity characteristics of the T67R variant of sperm whale myoglobin have been studied to assess the effects of introducing an arginine residue into the distal side of this protein, as occurs in the active site of heme peroxidases. The overall circular dichroism (CD) and NMR spectroscopic properties of various derivatives of the protein are little affected by the mutation. The mutant contains a high-spin ferric ion with a water molecule as the sixth ligand, which exhibits slightly enhanced acidity ($pK_a = 8.43 \pm 0.03$) with respect to the corresponding derivative of wild-type myoglobin ($pK_a = 8.60 \pm 0.04$). The presence of the distal arginine increases the affinity of the Fe^{III} center for azide ($K = (6.0 \pm 0.5) \times 10^4 M^{-1}$) and decreases that for imidazole ($K = 12.0 \pm 0.2 M^{-1}$), with respect to the wild-type protein ($K = (5.0 \pm 0.1) \times 10^4$ and $24.7 \pm 0.7 M^{-1}$, respectively). The peroxidase

activity of T67R and wild-type myoglobins has been studied with a group of phenolic substrates related to tyrosine. The mutant exhibits an increased rate of reaction with hydrogen peroxide ($k = 1550 \pm 10$ versus $760 \pm 10 M^{-1} s^{-1}$) and a generally increased peroxidase activity with respect to wild-type myoglobin. Relaxation measurements of proton nuclei of the phenolic substrates in the presence of either the T67R variant or the wild-type protein show that binding of these molecules occurs at distances of 8–10 Å from the iron center, that is, close to the heme pocket, except for p-cresol, which can approach the heme more closely and, therefore, probably enter into the distal cavity.

KEYWORDS:

heme proteins · metalloenzymes · O–O activation · oxidoreductases · phenol oxidation

Introduction

In recent years, site-directed mutagenesis has been intensively used as a tool to investigate the role of critical amino acid residues in the active site of myoglobins (Mbs) from various sources.^[1–8] Particularly interesting from the point of view of potential biotechnological applications are the experiments aimed at introducing catalytic activities into the Mb scaffold,^[9–14] to convert this oxygen storage protein into, for example, an oxidative enzyme with activity mimicking that of cytochrome P450s, peroxidases, or catalases. The most notable results in this field have been obtained in the stereoselective peroxygenase activity of Mb mutants against methylphenyl sulfide and styrene.^[11, 14] This activity is typical of chloroperoxidase, while classical peroxidases such as horseradish peroxidase (HRP) are poorly efficient in oxygen transfer reactions.^[15] It is not surprising, therefore, that the best performance in the peroxygenase reactions was exhibited by the His64 (E7) to Asp mutant, constructed to mimic the active site of chloroperoxidase.^[14] On the other hand, the peroxidase activity of site-directed Mb mutants, routinely measured against guaiacol as the substrate, is generally modest and this conclusion applies, in particular, to mutants that were constructed in an attempt to mimic the active site of cytochrome c peroxidase.^[10, 11] Somewhat more promising results have apparently been obtained with the multiple mutants resulting from random mutagenesis of Mb in the catalytic oxidation of 2,2'-azino-di-(3-ethyl)benzthiazoline-6-sulfonic acid (ABTS),^[9] but in that case it is difficult to assess the effects of the replacements, since none of the residues

introduced appears to play a direct role in the enhancement of activity.

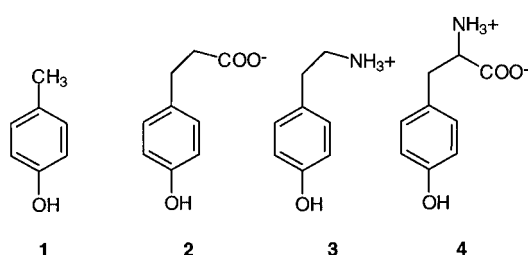
We have been interested for some time in synthetic and mechanistic aspects of peroxidase-catalyzed reactions with enzymes from various sources.^[16–20] More recently, we have explored the possibility of increasing the peroxidase activity of Mb through reconstitution of the apoprotein with chemically modified protohemins.^[21] The availability of the expression system for recombinant sperm whale Mb in *Escherichia coli*^[22] gives the opportunity to investigate in a systematic way the catalytic properties of Mb mutants with characteristics that may progressively enhance the efficiency of the proteins as peroxidase analogues. In this paper we report the detailed characterization and catalytic properties of the T67R Mb mutant. This

[a] Prof. L. Casella, Dr. C. Redaelli, Dr. E. Monzani, Dr. L. Santagostini
Dipartimento di Chimica Generale
Università di Pavia
Via Taramelli 12, 27100 Pavia (Italy)
Fax: (+39) 0382-528544
E-mail: bioinorg@unipv.it

[b] Prof. A. M. Sanangelantoni
Dipartimento di Scienze Ambientali
Università di Parma, 43100 Parma (Italy)

[c] Dr. R. Pierattelli, Prof. L. Banci
CERM and Dipartimento di Chimica
Università di Firenze
50019 Sesto Fiorentino, Firenze (Italy)

derivative was prepared previously, together with many other Mb mutants,^[2, 3] primarily with the end of explaining the unusual characteristics of Mb from *Aplysia limacina*.^[23] This protein lacks the distal histidine (E7) but contains an arginine residue (E10) that appears to be capable of stabilizing the binding of ligands to the iron center through hydrogen-bonding interactions from the guanidinium group.^[24] In spite of the fact that T67R Mb contains the key histidine and arginine residues which characterize the distal site of peroxidases,^[25, 26] no study of its potential catalytic activity has been performed before. On the other hand, the Mb mutants studied previously as peroxidase mimics lack a distal arginine and, therefore, we thought it of interest to investigate the catalytic activity of T67R Mb in typical peroxidase reactions, such as the oxidations of phenolic substrates 1–4. This information is important in assessing the effect of distal site alterations for the development of new Mb mutants with enhanced catalytic performance.



Results and Discussion

Characterization of the T67R mutant

The electronic spectra of the Fe^{III} form and other derivatives of T67R Mb are very similar to those of the corresponding derivatives of the wild-type (WT) protein (Table 1); this indicates that the distal site environment of Mb is little affected upon Thr67 → Arg substitution. In particular, T67R Mb contains a high-spin ferric ion with water as the sixth ligand in the unoxidized (met) form, and a five-coordinated ferrous ion in the reduced form.^[1] The presence of a distal Arg67 slightly increases the

affinity of the Fe^{III} center for a negatively charged ligand such as azide ($K = (6.0 \pm 0.5) \times 10^4$ for T67R Mb; $(5.0 \pm 0.1) \times 10^4 \text{ M}^{-1}$ for WT Mb) and decreases that for imidazole, which is significantly protonated at pH 6.0 ($K = 12.0 \pm 0.2$ for T67R Mb; $24.7 \pm 0.7 \text{ M}^{-1}$ for WT Mb). The investigation of the pH dependence of the optical properties of T67R and WT Mbs discloses two proton-dependent equilibria (Figure 1). Protonation of the proximal histidine was studied in the pH range of 4.5–7.^[27, 28] It can be

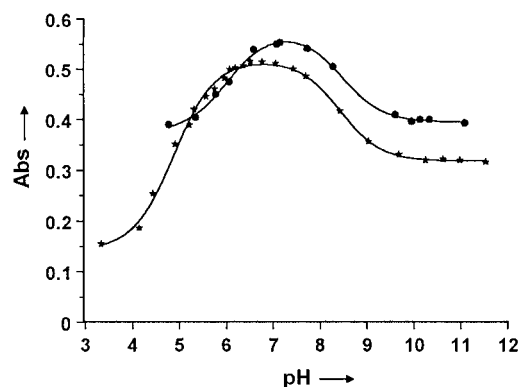


Figure 1. Acid-alkaline transitions observed for T67R Mb (*) and WT Mb (●) by spectrophotometric titrations. Continuous lines were obtained by fitting the experimental data for the proton dissociation equilibria according to Equation (10).

followed through the intensity changes of the Soret band and occurs with a pK of 4.89 ± 0.03 for T67R Mb and 6.03 ± 0.05 for WT Mb. The point mutation has a smaller effect on the proton dissociation equilibrium occurring in the alkaline pH range, ascribable to the deprotonation of iron-bound water [Eq. (1)]. Formation of the Fe^{III}–OH[−] species produces a red shift in the Soret band of the proteins (Table 1). The pK values that we found here for bound water are 8.43 ± 0.03 for T67R Mb and 8.60 ± 0.04 for WT Mb.



The far-UV circular dichroism (CD) spectrum of T67R Mb has a similar shape to that of WT Mb, although the fitting to secondary structure elements reveals a slightly reduced helical content (64.1% versus 71.4%, respectively). The CD ellipticity in the aromatic region and especially that in the Soret region, reflecting the coupling of electronic transitions of the porphyrin with transitions localized in residues in the heme environment,^[29] is quite similar for the two proteins; this confirms the maintenance of the overall globin fold in the mutant.

The 600 MHz ¹H NMR spectrum of T67R metMb is shown in Figure 2A. In the downfield region four three-proton intensity signals are observed, in addition to several one-proton signals. The spectrum is similar to that reported and assigned for WT Mb;^[30] this indicates that a similar coordination arrangement is present at the iron ion. Significantly, the broad signal shifted far downfield (103 ppm), which is probably due to the ring NH resonance of the axial histidine, also has a similar shift to that of the wild-type protein.

Table 1. Absorption spectral data [nm] for ferrous and ferric derivatives of T67R and WT Mbs.^[a]

Protein derivative	T67R Mb ^[b]		WT Mb ^[b]	
	Soret	visible	Soret	visible
Fe ^{II}	432 (118)	556 (13.2)	434 (115)	556 (11.8)
Fe ^{II} –O ₂	416 (122)	544 (13.7)	418 (128)	542 (13.6)
Fe ^{II} –CO	422 (164)	580 (13.3)	424 (187)	582 (13.3)
		540 (14.6)		540 (14.0)
Fe ^{III}	410 (149)	578 (12.4)	410 (157)	578 (12.2)
		504 (10.3)		504 (9.4)
Fe ^{III} –OH [−]	414 (100)	632 (3.9)	414 (117)	635 (3.6)
		540 (11.0)		540 (11.0)
Fe ^{III} –N ₃ [−]	422 (105)	584 (9.5)	420 (122)	586 (9.5)
		542 (10.7)		544 (12.7)
Fe ^{III} –imidazole	414 (123)	532 (13.7)	416 (129)	532 (12.7)

[a] Measured in 0.2 M phosphate buffer (pH 6.0). [b] Molar extinction coefficients [mM^{−1} cm^{−1}] are given in parentheses.

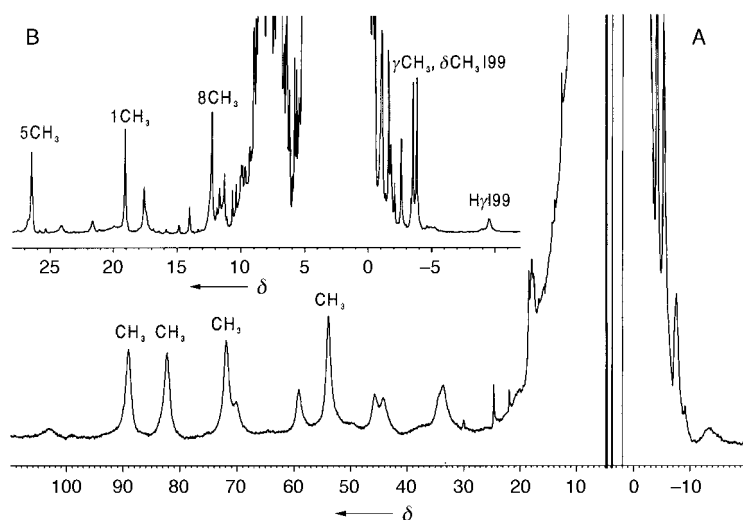


Figure 2. A) ^1H NMR spectrum (600 MHz) of T67R metMb. B) ^1H NMR spectrum (800 MHz) of T67R metMb-CN. The samples were in 20 mM tris(hydroxymethyl)aminomethane-HCl (Tris-HCl) buffer at pH 8, prepared in $^2\text{H}_2\text{O}/\text{H}_2\text{O}$ (1:9), at 25 °C.

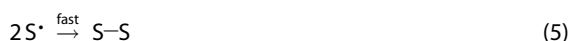
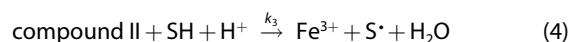
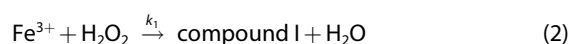
Addition of CN^- to the protein sample produces a low-spin state, characterized by narrower NMR lines that make two-dimensional experiments feasible (Figure 2B). Three of the downfield-shifted signals have a relative intensity of three and are assigned as heme methyl signals. A NOESY cross-peak between two of them locates the 1- CH_3 and 8- CH_3 pair. Each of the two signals shows a NOESY connectivity with at least one resonance of a COSY-detected vinyl and propionate spin system; this allows the identification of the 2-vinyl and the 7-propionate groups. The third methyl also shows NOESY cross-peaks to a propionate group; they must arise from the 5- CH_3 and 6-propionate groups. The remaining 4-vinyl group is assigned from the typical pattern in a COSY spectrum tailored to enhance fast relaxing signals. No resonance was found for the heme 3- CH_3 group, as it falls in the intense diamagnetic envelope of the signals. The assignment of the resolved upfield resonances is reported in Table 2. Minor peaks, with fractional intensities, can also be detected in the T67R metMb-CN spectrum between 20 and 25 ppm; these are most likely due to the minor heme orientational isomer of the protein.

Overall, the spectrum and the pattern of connectivities closely resemble those of the wild type metMb-CN^[31] and the metMb-CN derivatives of other point mutants.^[32] The NMR

spectra of the native and cyanide-bound species indicate that the mutation of Thr to Arg does not significantly perturb the heme electronic structure as well as its environment.

Kinetic studies

The peroxidase activities of WT and T67R Mbs were studied by considering the one-electron oxidation of phenolic substrates to phenoxy radicals. This reaction is typically performed by the two peroxidase intermediates known as compound I and compound II, according to the reaction scheme in Equations (2)–(5), where SH is the substrate, compound I a $\text{Fe}^{\text{IV}}=\text{O}/\text{R}^{\cdot+}$ species with a radical cation localized on the porphyrin or a protein residue, and compound II a $\text{Fe}^{\text{IV}}=\text{O}$ species.^[33, 34]



Myoglobin exhibits a weak peroxidase activity that is assumed to proceed through a similar mechanism.^[9, 35] The reaction with hydrogen peroxide, in the first step, is very fast for peroxidases ($k_1 \approx 10^7$)^[33] but drops dramatically for metMb ($k_1 \approx 10^2 \text{ M}^{-1} \text{ s}^{-1}$)^[36] and is accompanied by rather rapid protein degradation when excess oxidant is used. With Mb the radical site is distributed among different residues, including a tyrosine, a tryptophan (as a Trp peroxy radical), and a histidine residue (most likely distal histidine).^[37–42]

The kinetic constants for the formation of the active species in the first step [Eq. (2)], which we determined here at 25 °C and pH 6.0, show an appreciable increase from WT Mb ($k_1 = 760 \pm 10$) to T67R Mb ($k_1 = 1550 \pm 10 \text{ M}^{-1} \text{ s}^{-1}$). The Soret band of the intermediate is similarly shifted to longer wavelengths, with the maximum occurring near 422 nm for both Mb derivatives (Figure 3). The increase in k_1 for T67R Mb can be attributed to either of the following effects: (1) a slightly higher acidity of coordinated hydrogen peroxide, which favors the peroxide binding step, and/or (2) a positive contribution by the Arg67 mutation in the peroxide (heterolytic) cleavage step. The first effect would parallel the increased acidity observed for coordinated water in the mutant, the second one requires a direct interaction between the Arg67 side chain and the bound hydroperoxide anion, according to the classical peroxidase mechanism of Poulos and Kraut^[43] (Figure 4).

For Mb derivatives, the determination of the rate of reduction of compound I in the second step, k_2 , is technically difficult because this protein intermediate has optical features similar to compound II, but the process is probably very fast. In order to get an appreciation of the change in catalytic activity introduced by the T67R mutation, detailed steady-state kinetic experiments

Table 2. Assignment of upfield-shifted resonances of T67R metMb-CN and WT metMb-CN.

Residue	Position	Chemical shift	
		T67R Mb	WT Mb ^[a]
Ile99 (FG5)	C ₁ H'	-1.14	-1.91
	C ₇ H ₃	-3.56	-3.46
	C ₈ H ₃	-3.86	-3.83
	C ₇ H	-9.48	-9.60
Val68 (E11)	C ₆ H	-2.61	-2.55
	C ₇₁ H ₃	-0.59	-1.02
	C ₇₂ H ₃	-0.45	-0.89

[a] Data taken from ref. [61].

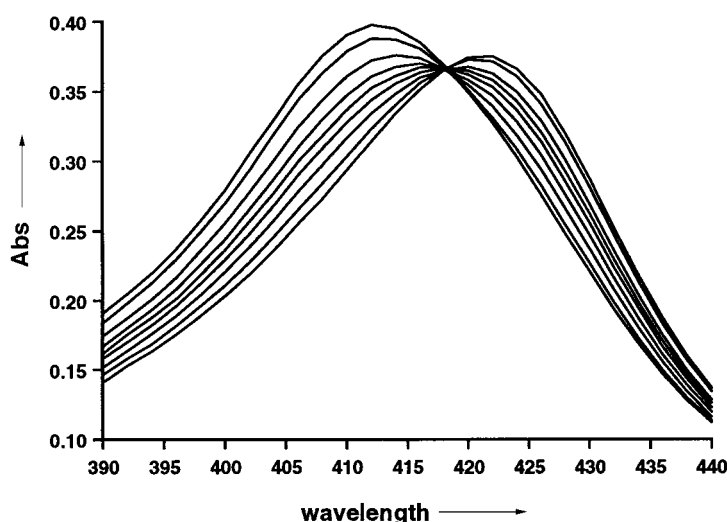


Figure 3. Rapid-scan spectra observed during the reaction between T67R Mb and excess hydrogen peroxide in 0.1 M phosphate buffer (pH 6.0) at 25 °C.

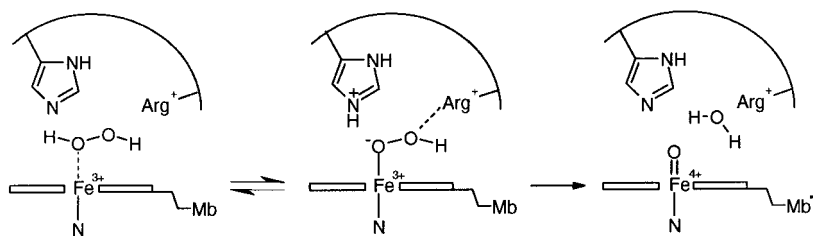
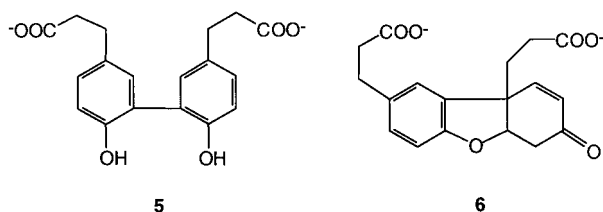


Figure 4. Elementary steps probably involved in compound I formation in T67R Mb, adapted from the work of Poulos and Kraut.^[43]

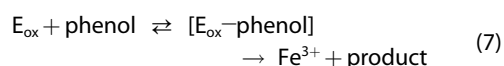
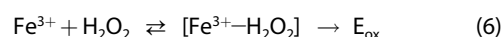
on the peroxidase activity towards the phenolic substrates 1–4 were performed.

It is known that the phenoxy radicals produced on phenol oxidation by the peroxidase/H₂O₂ systems according to the reactions shown in Equations (3) and (4) evolve in solution independently of the enzyme.^[18] Coupling of phenoxy radicals initially produces the two dimers, resulting from *ortho-ortho* coupling (α - α dimer) or *ortho-para* coupling followed by a cyclization rearrangement (Pummerer's ketone). Then, more complex mixtures of oligomeric products are obtained, which are difficult to analyze.^[44, 45] We have confirmed that the same behavior is followed in the peroxidase-like activity of T67R and WT Mbs by using high-pressure liquid chromatography (HPLC) separation and characterization of the dimeric products 5 (α - α dimer) and 6 (Pummerer's ketone), formed as the major products in the early stages of the reaction of 2. These are formed in a ratio



of 3:1 for 5:6, as with HRP. At reaction times longer than about 1 min the HPLC traces show the appearance of a progressively more complex pattern of peaks. However, by considering initial rates, only the formation of dimeric coupling products can be taken into account in the kinetics of the phenol oxidation reactions promoted by the Mbs and H₂O₂. Since the dimer composition is independent of the enzyme, the primary kinetic data for the oxidations of 1–4 were analyzed by using the apparent extinction coefficients for the dimers; these were conveniently determined from the peroxidase catalyzed reactions.^[18]

Assuming that reduction of compound I is a fast step, the catalytic scheme can be reduced to a simple bimolecular ping-pong mechanism of the type shown in Equations (6) and (7), where E_{ox} represents compound II.^[18]



The initial rate equation in these conditions is given by Equation (8), where [E₀] is the total protein concentration, *k*_{cat} corresponds to the maximum turnover rate of the protein, and *K*_M and *K*'_M are the Michaelis constants for the phenol and hydrogen peroxide, respectively.

$$r_0 = \frac{k_{\text{cat}}[\text{E}_0]}{1 + \frac{K'_M}{[\text{H}_2\text{O}_2]} + \frac{K_M}{[\text{phenol}]}} \quad (8)$$

Operating under saturating hydrogen peroxide conditions, the term *K*'_M/[H₂O₂] becomes negligible and the rate equation can be further simplified to conventional Michaelis–Menten kinetics.^[18] The kinetic parameters found for the catalytic reactions of WT and T67R Mbs are collected in Table 3.

The Arg 67 mutation produces an increase in the turnover rate of Mb in the oxidation of phenolic substrates 2 and 3. This may reflect a higher redox potential for compound II, that is, for the Fe⁴⁺=O/Fe³⁺ couple, in the T67R Mb mutant as a result of the increase of positive charge in the active site. On the other hand, *K*_M is sensitive to the charge present in the substrate side chain and this may affect the catalytic efficiency in opposite ways. For the anionic substrate 2, the activity of T67R Mb is enhanced by the marked reduction in *K*_M, which implies larger affinity for the protein containing the positively charged Arg 67 residue. On the other hand, for 3, which carries a positive charge, *K*_M is larger for T67R Mb than for WT Mb and this effect reduces the efficiency of the protein catalyst (in terms of *k*_{cat}/*K*_M). The behavior of the tyrosine enantiomers L-4 and D-4 in the catalytic oxidations by both Mb proteins is apparently contradictory, as for both systems remarkably small *K*_M constants, indicating strong bind-

Table 3. Kinetic parameters for the catalytic oxidation of phenols by T67R and WT Mbs and hydrogen peroxide.^[a]

Phenol	T67R Mb			WT Mb		
	k_{cat} [s ⁻¹]	K_{M} [mM]	$k_{\text{cat}}/K_{\text{M}}$ [M ⁻¹ s ⁻¹]	k_{cat} [s ⁻¹]	K_{M} [mM]	$k_{\text{cat}}/K_{\text{M}}$ [M ⁻¹ s ⁻¹]
1	[b]	[b]	1900 ± 200	[b]	[b]	4800 ± 200
2	2.3 ± 0.1	12 ± 2	190 ± 25	1.0 ± 0.1	72 ± 5	14 ± 0.4
3	1.4 ± 0.1	19 ± 4	76 ± 15	0.36 ± 0.02	4 ± 1	90 ± 11
L- 4	0.06 ± 0.03	0.50 ± 0.09	120 ± 15	0.16 ± 0.02	0.34 ± 0.13	470 ± 130
D- 4	0.06 ± 0.03	0.43 ± 0.05	140 ± 18	0.15 ± 0.02	0.41 ± 0.20	370 ± 120

[a] Measured in 0.1 M phosphate buffer (pH 6.0) at 25 °C. [b] See text.

ing to the proteins, are found together with a very inefficient electron transfer processes (small k_{cat}). Clearly, such a high affinity depends on some interaction between the charged groups present on these molecules and residues on the surface of the protein, but involves an unfavorable orientation of the phenol ring with respect to the heme. The NMR relaxation measurements, discussed below, indeed show that the phenol ring of these substrates binds far from the heme.

For *p*-cresol (**1**) the rate of the catalytic reactions is much higher than for the other phenolic substrates. With both the Mb protein catalysts, it was not possible to obtain the kinetic parameters k_{cat} and K_{M} for the reaction with this substrate. In fact, at high concentrations of **1**, even with hydrogen peroxide present in up to molar concentrations, the reaction rate was not independent of the oxidant concentration (further increase in H₂O₂ concentration causes a fast protein degradation). Therefore, the first step of the catalytic cycle, the formation of the active species, could not be considered as a fast step with respect to the substrate oxidation. The parameter $k_{\text{cat}}/K_{\text{M}}$ was obtained from the dependence of the rate on the *p*-cresol concentration in the low concentration range ($[1] < 4$ mM, $[\text{H}_2\text{O}_2] > 50$ mM). The observation of the spectrum of the iron(III) species during turnover confirms that in these conditions the slow step of the cycle is the formation of the active species. The lower $k_{\text{cat}}/K_{\text{M}}$ value determined for T67R Mb in this case could be due to changes of the individual parameters, since both of them can be affected by differences in the polarity of the protein active site.

The high oxidation rates for **1** depend on its low reduction potential (for the couple phenoxide radical/phenol), but also on the different mode of binding of this substrate (closer to the heme), that apparently further facilitates the electron transfer to the heme in the second step. Binding experiments of *p*-cresol to the Mbs show that, in fact, this substrate perturbs the Soret band of the proteins, even at relatively low concentrations, causing a small decrease in intensity without affecting the position of the band. However, the analysis of the absorbance changes as a function of *p*-cresol concentration is complicated, probably because more than a molecule of the phenol interacts with the proteins.

NMR relaxation of bound substrates

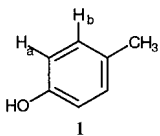
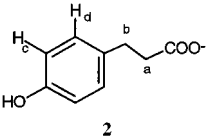
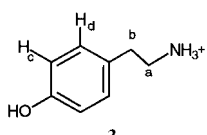
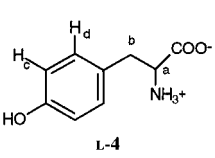
In order to gain an understanding of the protein–substrate interactions, we performed NMR relaxation measurements on substrates **1–4** in the presence of T67R and WT Mbs, where the

paramagnetic contribution by the high-spin Fe^{III} center can be exploited to estimate the distances of the substrate protons from the iron. As shown by the data collected in Table 4, *p*-cresol can approach the heme in both Mbs much more closely than the other phenolic substrates. Iron–proton distances in the range of 6.0–6.5 Å can only be accounted for by a disposition of the bound phenol partially inside the distal cavity (the protons of the porphyrin methyl groups are at 6.2 Å from the iron) and somewhat above the plane of the heme. This is not surprising since imidazole, with a comparable size, has access to the iron, and explains the larger reactivity of this substrate in the catalytic oxidation with respect to the other substrates. The binding of **2** and **3** to the Mbs occurs with iron–proton distances in the range of 8–10 Å, which is the same range commonly found for bound phenols in the active site of peroxidases.^[16, 18, 46, 47] Therefore, the low efficiency in the peroxidase activity of myoglobins does not depend on restrictions in the approach of the substrates to the heme. When these restrictions are operative, as in the case of L-**4** and D-**4**, a marked drop in reactivity is observed. A similar effect was previously found to control the peroxidase activity of chloroperoxidase towards phenolic substrates.^[18]

Concluding Remarks

The present study has explored the possibility of enhancing the peroxidase activity of myoglobin by site-directed mutagenesis. An important step in the construction of a peroxidase analogue is clearly engineering the active site of the protein with introduction of an arginine in the distal pocket, since this residue is highly conserved in peroxidases and plays a basic role in the peroxide activation process.^[33, 34, 43] As we have shown here, the Thr 67 → Arg mutation does not significantly affect the folding of the protein but does perturb the binding affinity of the iron center towards exogenous ligands and increases its reactivity with hydrogen peroxide. The mutant exhibits a modest but significant enhancement of peroxidase activity towards hydrogen peroxide and phenolic substrates. Since the mode of interaction of these substrates with the WT and T67R Mbs appears to be quite similar, the enhanced activity of the T67R mutant can be totally ascribed to the single-point mutation. Previous studies^[10, 11] have shown that other mutations of amino acids at the active site can slightly increase the reactivity towards peroxide. Other studies based on random mutagenesis of Mb have shown that an enhancement of peroxidase activity can be obtained by (unpredictable) modifications at the periphery of the active site.^[9] We are therefore confident that coupling the

Table 4. Substrate proton relaxation times and iron–proton distances for T67R Mb–phenol and WT Mb–phenol complexes.^[a]

Substrate	Proton [ppm]	T67R Mb		WT Mb	
		T_{1M} [s]	r [Å]	T_{1M} [s]	r [Å]
 1	CH ₃ 2.19	$(1.8 \pm 0.1) \times 10^{-3}$	6.6	$(1.8 \pm 0.1) \times 10^{-3}$	6.6
	(a) 6.77	$(1.5 \pm 0.1) \times 10^{-3}$	6.3	$(1.4 \pm 0.1) \times 10^{-3}$	6.3
	(b) 7.07	$(1.5 \pm 0.1) \times 10^{-3}$	6.3	$(1.4 \pm 0.1) \times 10^{-3}$	6.3
 2	(a) 2.30	$(2.1 \pm 0.1) \times 10^{-2}$	9.8	[b]	[b]
	(b) 2.77	$(2.0 \pm 0.1) \times 10^{-2}$	9.8		
	(c) 6.71	$(1.6 \pm 0.1) \times 10^{-2}$	9.4		
	(d) 7.03	$(2.0 \pm 0.1) \times 10^{-2}$	9.8		
 3	(a) 2.79	$(1.2 \pm 0.2) \times 10^{-2}$	8.6	$(1.1 \pm 0.1) \times 10^{-2}$	8.9
	(b) 3.09	$(9.0 \pm 0.6) \times 10^{-3}$	9.0	$(1.4 \pm 0.1) \times 10^{-2}$	9.1
	(c) 6.77	$(6.4 \pm 0.8) \times 10^{-3}$	8.1	$(8.7 \pm 0.8) \times 10^{-3}$	8.5
	(d) 7.07	$(7.4 \pm 0.9) \times 10^{-3}$	8.3	$(1.1 \pm 0.4) \times 10^{-2}$	8.7
 L-4	(a) 3.07	$(2.9 \pm 0.5) \times 10^{-2}$	10.4	$(1.0 \pm 0.1) \times 10^{-1}$	12.8
	(b) 3.88	$(5.7 \pm 1.0) \times 10^{-2}$	11.6	$(8.6 \pm 0.5) \times 10^{-2}$	12.4
	(c) 6.83	≈ 0.4	≈ 16	≈ 0.4	≈ 16
	(d) 7.11	≈ 0.6	≈ 17	≈ 0.3	≈ 15

[a] Measured in phosphate buffer (pH 6.0) at 25 °C. [b] See text.

present site-directed approach with techniques employing multiple-point mutations, like random mutagenesis,^[9] or cofactor modification^[21] will succeed in the conversion of myoglobin into an effective peroxidase.

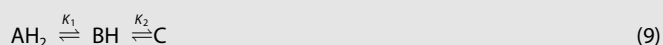
Experimental Section

Mutagenesis, expression, and protein purification: Site-directed mutagenesis of the Thr67 residue in the synthetic sperm whale gene^[22] was performed with the “LA PCR in vitro mutagenesis kit” (TaKaRa Biomedicals) through the polymerase chain reaction, by a set of oligonucleotides where the normal codon for Thr (ACC) had been substituted with that for Arg (CGT). Wild-type and mutant sperm whale Mbs were expressed in *E. coli* and purified according to the method described by Springer et al.^[22] Purity of the proteins was checked by sodium dodecylsulfate polyacrylamide gel electrophoresis (SDS-PAGE) analysis and monitoring the absorbance ratio A_{Soret}/A_{280} , which was above 3. Absorption coefficients were determined by using the pyridine hemochromogen assay.^[48] The expression of both Mbs yields the proteins in the Fe^{II}–O₂ form; the Fe^{III} species was obtained by treating the proteins with diluted H₃PO₄ until the pH value was 3.5 followed by addition of diluted NaOH to raise the pH value to 8. The acid treatment remarkably increases the autoxidation rate of myoglobins.^[49]

Spectroscopic characterization: The UV-Vis spectra of WT and T67R Mbs were recorded in sodium phosphate buffer (pH 6.0; $\mu=0.2\text{M}$), with a HP8452A diode array spectrophotometer. The various derivatives of the proteins were obtained as described previously.^[21] CD spectra were measured with a Jasco J710 dichrograph. Determination of secondary structure contributions was performed by fitting of the CD spectra with software available from Jasco.

Spectrophotometric acid–base titrations: These experiments were performed with solutions of WT and T67R Mbs ($\approx 4\ \mu\text{M}$) at a series of

pH values in the range between 3.5 and 11.5 by using a thermostated cell with a path length of 1 cm. Typically, the protein solution, initially in sodium phosphate buffer (pH 5.0; $\mu=0.2\text{M}$) at $25.0 \pm 0.1\ ^\circ\text{C}$, was brought to the given pH value by small additions of phosphoric acid or sodium hydroxide solutions. After recording each spectrum, the pH value was measured again. The pK values were obtained from the absorbance variations of the Soret band of the protein against the pH values, after correcting for dilution. Fitting of the data was performed considering the successive dissociation equilibria [Eq. (9)] through Equation (10), where Z is the absorbance at each pH value, and A – C are the absorbancies of the acid (AH₂), neutral (BH), and basic (C) forms of the protein, respectively.



$$Z = \frac{A + B \times 10^{(\text{pH}-\text{p}K_1)} + C \times 10^{(2\text{pH}-\text{p}K_1-\text{p}K_2)}}{1 + 10^{(\text{pH}-\text{p}K_1)} + 10^{(2\text{pH}-\text{p}K_1-\text{p}K_2)}} \quad (10)$$

Binding experiments: The equilibrium constants for the association of azide and imidazole to the WT and T67R Mb forms were determined by spectrophotometric titrations in 0.2M phosphate buffer (pH 6.0) at $25.0 \pm 0.1\ ^\circ\text{C}$ by using a thermostated optical cell with a path length of 1 cm, as described previously.^[21]

HPLC analysis of phenolic dimers: HPLC analyses of the oxidation products of **2** were performed at room temperature with an AKTA purifier (Pharmacia Biotech) and a Supelco LC18 reverse-phase semipreparative column (5 micron). The eluates were monitored at two wavelengths, $\lambda_1=280\ \text{nm}$ and $\lambda_2=200\ \text{nm}$. The solvents chosen for the separation were: solvent A, 0.1% trifluoroacetic acid (TFA) in distilled water and solvent B, 0.1% TFA in CH₃CN; gradient runs were performed with a flow rate of $6\ \text{mL}\ \text{min}^{-1}$. The elution was performed for 2.5 column volumes with 10% solvent B and then with a gradient up to 55% solvent B in 7 column volumes.

In a typical experiment, a solution of 10 mM **2** and 1 μM WT or T67R Mb in 0.2M phosphate buffer (pH 6.0) at $25.0 \pm 0.1\ ^\circ\text{C}$ was treated

with 11.5 mM hydrogen peroxide. After 1 min, a small volume of the reaction mixture was injected into the column. Two major products, with retention times of 12.7 and 13.0 min, were separated from the prominent peak of unreacted phenol at 7.7 min and collected. A few other smaller peaks eluted at longer times. ^1H NMR spectroscopy and mass spectrometry analysis indicate that the peak at 12.7 min corresponds to the α - α dimer (**5**; 3-[5'-(2-carboxy-ethyl)-6,2'-dihydroxy-biphenyl-3-yl]-propionic acid) while the peak at 13.0 min corresponds to the Pummerer's ketone (**6**; 3-[2-(2-carboxy-ethyl)-7-oxo-6,7-dihydro-5aH-dibenzofuran-9a-yl]-propionic acid).

Kinetic studies: Comparative kinetic experiments on WT and T67R Mbs were performed in 0.2 M phosphate buffer (pH 6.0) at 25.0 ± 0.1 °C, with the thermostated and magnetically stirred optical cell of 1 cm path length. The reactions were followed through the increase of absorbance at 300 nm in the initial phase (typically 5–10 s) due to the formation of phenol dimerization products.^[18] In order to reduce the noise in the absorbance readings, the difference in absorbance between 300 and 500 nm, where the absorption of reagents and products is negligible, was monitored. In preliminary experiments, the linearity between oxidation rates and Mb catalysts concentration was established. Relatively high concentrations of the phenols (30–60 mM, except for L- and D-tyrosine, for which the solubility limit is about 2 mM) and hydrogen peroxide (20 mM) were used, while the protein concentration was varied from 0–1.5 μM . The plots were found to be linear for both WT and T67R Mbs (data not shown). These experiments also enabled us to find conditions of protein catalyst concentrations that make the noncatalytic phenol oxidation reactions negligible.

The steady-state kinetics of oxidation of the phenolic substrates **1–4** by hydrogen peroxide were studied as a function of substrate concentration under saturating hydrogen peroxide conditions. These conditions were established for the phenolic derivatives **2**, **3**, L-**4**, and D-**4** by studying the rate dependence of the catalytic oxidation at high substrate concentration (typically 50 mM; about 1.5 mM for L- and D-tyrosine) as a function of hydrogen peroxide concentration (0.05–40 mM); with **1**, the saturation of H_2O_2 concentration could be obtained only at low (4 mM) substrate concentration. The Mb catalyst concentration in these experiments was kept at 0.1 μM for **1** and 1 μM for **2–4**. The experiments at variable substrate concentrations were carried out in the following conditions: for **1**, [protein] = 0.1 μM , [H_2O_2] = 46 mM, [substrate] = 0.3–4 mM; for **2**, [protein] = 0.5 μM , [H_2O_2] = 11.5 mM, [substrate] = 2–75 mM; for **3**, [protein] = 1 μM , [H_2O_2] = 15 mM, [substrate] = 1–50 mM; for L-**4** and D-**4**, [protein] = 2 μM , [H_2O_2] = 5 mM, [substrate] = 0.1–1.9 mM. With **2**, **3**, L-**4**, and D-**4** the kinetics exhibited substrate saturation behavior and the kinetic parameters k_{cat} and K_{M} were calculated through the fitting of the rate versus substrate concentration data.^[50] Conversion of rate data from absorbance s^{-1} into mol s^{-1} units was obtained by using the difference in molar extinction coefficient ($\Delta\epsilon$) between the mixture of dimeric products and the phenolic substrates at 300 nm, as described previously.^[18] The following $\Delta\epsilon$ values were determined from the enzymatic oxidation of **1–4** by HRP and hydrogen peroxide in the same conditions and used in the calculations: for **1** $\Delta\epsilon = 2350$, for **2** 1950, for **3** 1460, for L-**4** and D-**4** $1350 \text{ M}^{-1} \text{ cm}^{-1}$.

The second-order catalytic constant for the reaction between wild type or T67R Mb and hydrogen peroxide was determined with a Model RS-1000 Applied Photophysics stopped-flow apparatus thermostated at 25.0 ± 0.1 °C. The reactions were followed by monitoring the absorbance changes of the proteins (5.5 μM) with time (readings every 0.1 s) in the range of 390–440 nm; a variable excess of hydrogen peroxide (50 μM –1.5 mM) was used in 0.1 M phosphate buffer (pH 6.0). The active species formation follows a first-order behavior. The observed constant (k_{obs}) depends on the hydrogen

peroxide concentration. The replots of k_{obs} versus H_2O_2 concentration were linear and the slope gave the catalytic constants.

^1H NMR spectroscopy: Proton NMR spectra of the Fe^{III} forms of T67R Mb were recorded with a Bruker AVANCE 600 spectrometer, operating at 600.13 MHz and equipped with a high-power probe, on solutions of the protein in 20 mM Tris-HCl buffer (pH 8.0) prepared in $^2\text{H}_2\text{O}/\text{H}_2\text{O}$ (1:9) and containing 1 mM ethylenediaminetetraacetate (EDTA). The cyanide adduct of T67R Mb (T67R metMb-CN) was obtained by addition of excess KCN to a solution of the protein in the same buffer. The spectra of this adduct were recorded on a Bruker AVANCE 800 spectrometer, operating at 800.13 MHz, with a standard TXI probe. Two-dimensional NOESY,^[51] TOCSY,^[52] and COSY^[53] maps were recorded by collecting 512 experiments over the 60 ppm spectral width and by using 2048 data points. All the spectra above were acquired in the phase-sensitive mode^[54] with standard pulse sequences and processed by using XWINNMR Bruker software. All the matrices recorded were zero-filled up to either 2048×1024 or 2048×512 data points. NOESY spectra were collected at both 25 and 35 °C.

NMR relaxation measurements: The T_1 relaxation times for the protons of substrates **1–4** in the presence of variable amounts of WT or T67R Mbs were determined with a Bruker AVANCE 400 spectrometer operating at 400.13 MHz, by using the standard inversion recovery method.^[55] Solutions of the substrates were prepared in deuterated 0.2 M sodium phosphate buffer (pH 6.0; the deuterium isotopic effect was neglected), with the addition of a small quantity of EDTA to remove metal impurities, and contained different concentrations of WT or T67R Mb (0–0.2 mM). The concentrations of the substrates in these solutions were 30 mM for **1** and **2**, 40 mM for **3**, and 1 mM for L-**4**. The relaxation rate of the protons of substrate molecules interacting with the Mb, $T_{1\text{b}}$, can be calculated from the experimental relaxation rate, $T_{1\text{obs}}$, according to Equation (11), where $T_{1\text{f}}$ is the T_1 value for free substrate, E_0 and S_0 are the initial protein and substrate concentrations, respectively, and K_{D} is the dissociation constant for the Mb–substrate complex.^[56]

$$\frac{1}{T_{1\text{obs}}} = \left[\frac{1}{T_{1\text{b}}} - \frac{1}{T_{1\text{f}}} \right] \frac{E_0}{K_{\text{D}} + S_0} + \frac{1}{T_{1\text{f}}} \quad (11)$$

The K_{D} values for substrates **1–4** were assumed coincident with the K_{M} values deduced from kinetic experiments. $1/T_{1\text{b}}$ is given by the relaxation rate of the substrate nuclei when the substrate is bound to the protein in the diamagnetic form ($1/T_{1\text{d}}$) and by the rate determined by the interaction of the substrate with the paramagnetic metal ion ($1/T_{1\text{M}}$). Relaxation measurements, performed at two different temperatures (25 and 35 °C), showed that no exchange contribution to relaxation is present.^[56, 57] The diamagnetic contribution to relaxation was estimated by performing relaxation measurements of the substrate protons in the presence of variable amounts of the cyanide adduct of the protein, assuming a K_{D} value similar to that of metMb for metMb-CN. The reduced S value (1/2 instead of 5/2) and the smaller τ_{c} value of this protein derivative induces a much smaller $1/T_{1\text{b}}$ value, which can be considered as an upper limit of $1/T_{1\text{d}}$. The paramagnetic contribution to relaxation originates only from dipolar relaxation, according to the Solomon-Bloembergen equation [Eq. (12)], where γ_i is the gyromagnetic ratio of the resonating nucleus, g_{e} is the g factor of the free electron, r is the distance of the nucleus from the Fe^{III} center, and ω_I and ω_S are the Larmor frequencies of I and S , respectively.^[58, 59]

$$T_{1\text{M}}^{-1} = \frac{2}{15} \left(\frac{\mu_0}{4\pi} \right)^2 \frac{\gamma_i^2 g_{\text{e}}^2 \mu_{\text{B}}^2 S(S+1)}{r^6} \left[\frac{7\tau_{\text{c}}}{1 + \omega_I^2 \tau_{\text{c}}^2} + \frac{3\tau_{\text{c}}}{1 + \omega_S^2 \tau_{\text{c}}^2} \right] \quad (12)$$

The correlation time τ_{c} for the paramagnetic contribution to the nuclear relaxation, in the case of slowly rotating molecules, is

dominated by the electron relaxation rate, τ_s . This has been reported to be 5×10^{-11} s for high-spin Fe^{III} myoglobin,^[60] and we used the same value for the WT and T67R Mbs.

In the case of 2, the plot of $T_{1\text{obs}}$ versus $E_0/(K_D + S)$ measured in the presence of WT Mb was not found to be linear, instead the slope decreased at high protein concentration; thus, the T_{1b} value could not be estimated.

We are indebted with Dr. John S. Olson (Rice University) for providing the cDNA of sperm whale myoglobin. This work was supported by funds from PRIN (Progetto di ricerca di interesse nazionale) of the Italian MURST and the EC (Contract no.: FMRXCT980218). The support from the Florence Large Scale Facility PARABIO (EC contract no.: HPRICT9900009) and from COST is also acknowledged.

- [1] B. A. Springer, S. G. Sligar, J. S. Olson, G. N. Phillips, Jr., *Chem. Rev.* **1994**, *94*, 699–714.
- [2] S. J. Smerdon, S. Krzywda, A. M. Brzozowski, G. J. Davies, A. J. Wilkinson, A. Brancaccio, F. Cutruzzolà, C. Travaglini Allocatelli, M. Brunori, T. Li, R. E. Brantley, Jr., T. E. Carver, R. F. Eich, E. Singleton, J. S. Olson, *Biochemistry* **1995**, *34*, 8715–8725.
- [3] A. Brancaccio, F. Cutruzzolà, C. Travaglini Allocatelli, M. Brunori, S. J. Smerdon, A. J. Wilkinson, Y. Dou, D. Keenan, M. Ikeda-Saito, R. E. Brantley, Jr., J. S. Olson, *J. Biol. Chem.* **1994**, *269*, 13843–13853.
- [4] T. E. Zewert, H. B. Gray, I. Bertini, *J. Am. Chem. Soc.* **1994**, *116*, 1169–1173.
- [5] E. Lloyd, D. L. Burk, J. C. Ferrer, R. Maurus, J. Doran, P. R. Carey, G. D. Brayer, A. G. Mauk, *Biochemistry* **1996**, *35*, 11901–11912.
- [6] E. Lloyd, D. P. Hildebrand, K. M. Tu, A. G. Mauk, *J. Am. Chem. Soc.* **1995**, *117*, 6434–6438.
- [7] B. R. Van Dyke, P. Saltman, F. A. Armstrong, *J. Am. Chem. Soc.* **1996**, *118*, 3490–3492.
- [8] S. Hirota, T. Li, G. N. Phillips, Jr., J. S. Olson, M. Mukai, T. Kitagawa, *J. Am. Chem. Soc.* **1996**, *118*, 7845–7846.
- [9] L. Wan, M. B. Twitchett, L. D. Eltis, A. G. Mauk, M. Smith, *Proc. Natl. Acad. Sci. USA* **1998**, *95*, 12825–12831.
- [10] S. Ozaki, T. Matsui, Y. Watanabe, *J. Am. Chem. Soc.* **1996**, *118*, 9784–9785.
- [11] S. Ozaki, I. Hara, T. Matsui, Y. Watanabe, *Biochemistry* **2001**, *40*, 1044–1052.
- [12] S. Adachi, S. Nagano, K. Ishimori, Y. Watanabe, I. Morishima, T. Egawa, T. Kitagawa, R. Makino, *Biochemistry* **1993**, *32*, 241–252.
- [13] T. Matsui, S. Nagano, K. Ishimori, Y. Watanabe, I. Morishima, *Biochemistry* **1996**, *35*, 13118–13124.
- [14] T. Matsui, S. Ozaki, Y. Watanabe, *J. Am. Chem. Soc.* **1999**, *121*, 9952–9957.
- [15] M. P. J. Van Deurzen, F. van Rantwijk, R. A. Sheldon, *Tetrahedron* **1997**, *39*, 13183–13220.
- [16] L. Casella, M. Gullotti, S. Poli, M. Bonfà, R. P. Ferrari, A. Marchesini, *Biochem. J.* **1991**, *279*, 245–250.
- [17] L. Casella, M. Gullotti, R. Ghezzi, S. Poli, T. Beringhelli, S. Colonna, G. Carrea, *Biochemistry* **1992**, *31*, 9451–9459.
- [18] L. Casella, S. Poli, M. Gullotti, C. Selvaggini, T. Beringhelli, A. Marchesini, *Biochemistry* **1994**, *33*, 6377–6386.
- [19] L. Casella, E. Monzani, M. Gullotti, E. Santelli, S. Poli, T. Beringhelli, *Gazz. Chim. Ital.* **1996**, *126*, 121–125.
- [20] E. Monzani, A. L. Gatti, A. Profumo, L. Casella, M. Gullotti, *Biochemistry* **1997**, *36*, 1918–1926.
- [21] E. Monzani, G. Alzuet, L. Casella, C. Redaelli, C. Bassani, A. M. Sanangelantoni, M. Gullotti, L. De Gioia, L. Santagostini, F. Chillemi, *Biochemistry* **2000**, *39*, 9571–9582.
- [22] B. A. Springer, S. G. Sligar, *Proc. Natl. Acad. Sci. USA* **1987**, *84*, 8961–8965.
- [23] M. Bolognesi, S. Onesti, G. Gatti, A. Coda, P. Ascenzi, M. Brunori, *J. Mol. Biol.* **1989**, *205*, 529–544.
- [24] E. Conti, C. Moser, M. Rizzi, A. Mattevi, C. Lionetti, A. Coda, P. Ascenzi, M. Brunori, M. Bolognesi, *J. Mol. Biol.* **1993**, *233*, 498–508.
- [25] L. Banci, *J. Biotechnol.* **1997**, *53*, 253–263.
- [26] H. Li, T. L. Poulos, *Structure* **1994**, *2*, 461–464.
- [27] G. M. Giacometti, T. G. Traylor, P. Ascenzi, M. Brunori, E. Antonini, *J. Biol. Chem.* **1977**, *252*, 7447–7448.
- [28] M. Coletta, P. Ascenzi, T. G. Traylor, M. Brunori, *J. Biol. Chem.* **1985**, *260*, 4151–4155.
- [29] Y. P. Myer, A. Pande in *The Porphyrins*, Vol. 3 (Ed.: D. Dolphin), Academic Press, New York, **1978**, Chap. 6.
- [30] G. N. LaMar, D. L. Budd, K. M. Smith, K. C. Langry, *J. Am. Chem. Soc.* **1980**, *102*, 1822–1827.
- [31] Y. Yamamoto, A. Osawa, Y. Ynoue, R. Chujo, T. Suzuki, *FEBS Lett.* **1989**, *247*, 263–267.
- [32] J. Qin, G. N. LaMar, F. Cutruzzola, C. Travaglini Allocatelli, A. Brancaccio, M. Brunori, *Biophys. J.* **1993**, *65*, 2178–2190.
- [33] H. Anni, T. Yonetani, *Met. Ions Biol. Syst.* **1992**, *28*, 219–241.
- [34] H. B. Dunford, *Heme Peroxidases*, Wiley, New York, **1999**.
- [35] M. B. Grisham, J. Everse in *Peroxidases in Chemistry and Biology*, Vol. I (Eds.: J. Everse, K. E. Everse, M. B. Grisham), CRC, Boca Raton, FL, **1991**, pp. 335–344.
- [36] T. Yonetani, H. Schleyer, *J. Biol. Chem.* **1967**, *242*, 1974–1979.
- [37] G. N. Phillips, Jr., R. M. Arduini, B. A. Springer, S. G. Sligar, *Proteins: Struct. Funct. Genet.* **1990**, *7*, 358–365.
- [38] C. W. Fenwick, A. M. English, *J. Am. Chem. Soc.* **1996**, *118*, 12236–12237.
- [39] J. A. DeGray, M. R. Gunther, R. Tschirret-Guth, P. R. Ortiz de Montellano, R. P. Mason, *J. Biol. Chem.* **1997**, *272*, 2359–2362.
- [40] K. Sugiyama, R. J. Highet, A. Woods, R. J. Cotter, Y. Osawa, *Proc. Natl. Acad. Sci. USA* **1997**, *94*, 796–801.
- [41] M. R. Gunther, R. A. Tschirret-Guth, H. E. Witkowska, Y. C. Fann, D. P. Barr, P. R. Ortiz de Montellano, R. P. Mason, *Biochem. J.* **1998**, *330*, 1293–1299.
- [42] K. Tsukahara, K. Kiguchi, M. Matsui, N. Kubota, R. Arakawa, T. Sakurai, *J. Biol. Inorg. Chem.* **2000**, *5*, 765–773.
- [43] T. L. Poulos, J. Kraut, *J. Biol. Chem.* **1980**, *255*, 8199–8205.
- [44] T. Michon, M. Chenu, N. Kellershon, M. Desmadril, J. Guégen, *Biochemistry* **1997**, *36*, 8504–8513.
- [45] A. Bertazzo, C. V. L. Costa, G. Allegri, M. Schiavolini, D. Favretto, P. Traldi, *Rapid Commun. Mass Spectrom.* **1999**, *13*, 542–547.
- [46] J. Sakurada, S. Takahashi, T. Hosoya, *J. Biol. Chem.* **1986**, *261*, 9657–9662.
- [47] S. Modi, D. V. Behere, S. Mitra, *Biochim. Biophys. Acta* **1989**, *996*, 214–225.
- [48] E. Antonini, M. Brunori, *Hemoglobin and Myoglobin in their Reactions with Ligands*, North-Holland Publishing Co., Amsterdam, **1971**.
- [49] R. J. Brantley, Jr., S. J. Smerdon, A. J. Wilkinson, E. W. Singleton, J. S. Olson, *J. Biol. Chem.* **1993**, *268*, 6995–7010.
- [50] I. H. Segel, *Enzyme Kinetics*, Wiley, New York, **1975**.
- [51] S. Macura, K. Wüthrich, R. R. Ernst, *J. Magn. Reson.* **1982**, *47*, 351–357.
- [52] A. Bax, D. G. Davis, *J. Magn. Reson.* **1985**, *65*, 355–360.
- [53] A. Bax, R. Freeman, G. Morris, *J. Magn. Reson.* **1985**, *42*, 164–168.
- [54] D. Marion, K. Wüthrich, *Biochem. Biophys. Res. Commun.* **1983**, *113*, 967–974.
- [55] R. L. Vold, J. S. Waugh, M. P. Klein, D. E. Phelps, *J. Chem. Phys.* **1968**, *48*, 3831–3832.
- [56] L. Banci, I. Bertini, C. Luchinat, *Nuclear and Electron Relaxation. The Magnetic Nucleus-Unpaired Electron Coupling in Solution*, VCH, Weinheim, **1991**.
- [57] I. Bertini, C. Luchinat, *Coord. Chem. Rev.* **1996**, *150*, 111–130.
- [58] I. Solomon, *Physiol. Rev.* **1955**, *99*, 559–565.
- [59] N. Bloembergen, *J. Chem. Phys.* **1957**, *27*, 572–573.
- [60] S. Modi, D. V. Behere, S. Mitra, *J. Inorg. Biochem.* **1990**, *38*, 17–25.
- [61] S. D. Emerson, G. N. La Mar, *Biochemistry* **1990**, *29*, 1545–1556.

Received: March 28, 2001

Revised version: October 10, 2001 [F225]